An $N^2 \log N$ Back-Projection Algorithm for SAR Image Formation

Shu Xiao[†] David C. Munson, Jr.[†] Samit Basu[*] Yoram Bresler[†]

[†] University of Illinois at Urbana-Champaign
1308 W. Main St., Urbana, IL 61801
s-xiao@ifp.uiuc.edu

[*]CT Program IEL, General Electric
Niskayuna, NY 12309
basu@crd.ge.com

Abstract

We propose a fast algorithm for far-field SAR imaging based on a new fast back-projection algorithm developed for tomography. We also modify the algorithm for the near-field scenario. The fast back-projection algorithm for SAR has computational complexity $O(N^2 log N)$. Compared to traditional FFT-based methods, our new algorithm has potential advantages: the new algorithm does not need frequency-domain interpolation, which becomes complex for the wide-angle case; the new approach is applicable to the near-field scenario, taking into account wavefront curvature; and the back-projection algorithm can be easily adapted to parallel computing architectures. For some scenarios of interest, the computational cost of the new back-projection approach is similar to or less than that for FFT-based algorithms.

1. Introduction

Our approach for SAR imaging is motivated by the recently proposed fast back-projection algorithms in tomography [1][2]. In spotlight-mode SAR, the physical antenna is steered to illuminate the same terrain area while the radar platform is moving along the flight path. Munson *et. al.* connected spotlight-mode SAR and computer-aided tomography (CAT) in 1983 [3]. In their paper, it was shown that in the far-field scenario, spotlight-mode SAR imaging is essentially a narrow-band version of CAT. After quadrature demodulation, the SAR return signals are approximately samples of 1-D Fourier transforms of projections of the scene patch, which are also are polar-grid samples of the 2-D FT of the scene. Thus, the filtered back-projection method, which originated in tomography, can be used to reconstruct a SAR image. The disadvantage of this inversion algorithm is its computational expense. For an $N \times N$ image, back-projection has $O(N^3)$ complexity. Traditional SAR imaging is FFT-based. With that method, the 2-D polar grid FFT data are first interpolated onto a Cartesian grid and the scene is reconstructed by a simple inverse 2-D FFT. This method is not applicable in the near-field scenario, since the plane-wave assumption breaks down and wavefront curvature must be taken into account. Another difficulty of the FFT-based method is that interpolation errors in the frequency-domain cause error propagation over the entire image, which could be a problem with a wide data collection angle. It has been proved that polar-to-Cartesian interpolation using a 2-D periodic sinc-kernel interpolator with Jacobian weighting followed by a 2-D inverse FFT is equivalent to the filtered back-projection algorithm [4]. A standard implementation of this interpolator would have complexity $O(N^4)$ for an $N \times N$ image. The FBP algorithm is a fast way of implementing the interpolation followed by an inverse FFT. A more sophisticated algorithm; the $\omega - k$ algorithm [5][6], accounts for wavefront curvature, but it still requires frequency-domain interpolation, referred to as "Stolt interpolation". The filtered back-projection algorithm potentially eliminates all the above problems: it avoids frequency-domain interpolation, it can be modified for the near-field scenario; furthermore, it is compatible with larger variety of auto-focus algorithms and it is easily adapted to parallel computing architectures. Back-projection in SAR would hold promise if its computational complexity could be decreased to that of a 2-D FFT. We propose such a fast back-projection algorithm in this paper.

In Section 2 we review recently proposed fast back-projection algorithm in CT and SAR. In Section 3 we present the algorithm we have developed for SAR image formation in the far-field scenario, and show some simulation results. In Section 4 we briefly describe the modified fast algorithm for the near-field scenarios and present simulations.

2 Review of fast algorithms

Boag and Bresler have proposed a novel fast reprojection algorithm [1] in tomography. Reprojection means to

obtain a set of parallel beam projections at view angles $\theta_i \in [0, \pi), i = 1, \cdots P$ given a 2-D image [7]. Direct algorithms for reprojection require $O(N^3)$ operations to generate N projections for an $N \times N$ image. The fast reprojection algorithm proposed in [1] utilizes the angular bandlimit property of the sinogram [8][9]. Let $f(r, \theta)$ be the projection function (Radon transform) of image $g(x, y)$ in variables r and θ, and $F(\omega_r, \omega_\theta)$ be its 2-D Fourier transform. $F(\omega_r, \omega_\theta)$ is a line spectrum in θ since $f(r, \theta)$ is periodic with respect to θ. The angular bandlimit property states:

Theorem 1 *If $f(r, \theta)$ is supported in $|r| < R$ and $F(\omega_r, \omega_\theta)$ essentially vanishes for $|\omega_r| > B_r$, then $F(\omega_r, \omega_\theta)$ essentially vanishes for $|\omega_\theta| > [RB_r] + 1$.*

This implies that for a subimage of half size, as in Fig. 1, the angular frequency support is halved, and hence the Nyquist sampling rate in θ is also halved. Therefore, to calculate P projections of the subimages, it is enough to calculate half the number of projections and then angularly interpolate them to P angles. Reprojection of the whole image is simply a shifted summation of the reprojections of the subimages [7][10]. Recursively using the domain decomposition, the computational requirement for fast reprojection is $O(N^2 \log N)$.

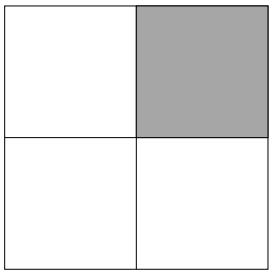

original image

Figure 1. Original image and its subimages.

Basu and Bresler further proposed a fast back-projection algorithm [2][11] based on the fast reprojection algorithm. Their idea is: since the back-projection operator is the adjoint operator of reprojection, the reprojection process can be inverted by its adjoint operator to obtain a fast back-projection algorithm with the same approximation errors. The fast hierarchical back-projection of P projections consists of several steps: shift and truncate the projection data of the original image to correspond to the data for each of the subimages, angularly filter and decimate the projection data to yield four sets of $\frac{P}{2}$ projections, and back-project the reduced number of filtered projections to obtain subimages. The reconstructed image is formed by combining all the subimages. The algorithm has $O(N^2 \log N)$ complexity when applied recursively. Earlier, McCorkle proposed a fast algorithm [12] with a similar approach, but resulting in larger errors.

3 Fast algorithm in far-field SAR scenario

In a spotlight mode SAR, the radar is assumed to illuminate the same scene patch while transmitting a sequence of pulses along the flight path. The following assumptions are made in the imaging procedure: first, we ignore the radar height h by setting $h = 0$. Second, the standard stop-and-go model of radar motion is assumed. This is a good model in practice, since the velocity of the airplane is neglectable compared to the velocity of light. Let the radar transmit a linear FM chirp pulse $\mathrm{Re}\{s(t)\}$, with

$$s(t) = \begin{cases} e^{j(\omega_0 t + \alpha t^2)} & |t| \le \frac{T}{2} \\ 0 & \text{otherwise} \end{cases} \quad (1)$$

where ω_0 is the RF carrier frequency and 2α is the FM rate. In the far-field SAR scenario, after quadrature demodulation, the return signals can be approximated as 1-D FTs of projections of the terrain patch [3][13]. See Fig. 2 for the typical far-field SAR data region. Each solid line in the figure represents complex data collected by one transmitting and receiving process. From the projection-slice theorem, the return data are also samples of the 2-D polar-grid Fourier transform of the scene, which allows us to first interpolate the polar-grid FT data to a Cartesian-grid and then 2-D inverse Fourier transform to form the terrain image. Similar algorithms, called Fourier Reconstruction Algorithms, are also used in tomography [14]–[16]. The FFT-based algorithms are fast to implement, and under some circumstances, the data collection angle θ in Fig. 2 is quite small (e.g. 3^o) such that the polar-grid data is already very close to Cartesian. The FFT-based algorithm can be accurate in this case, even with a simple interpolator. As the viewing angle increases, the performance of FFT-based algorithms can be disappointing unless a very high quality interpolator is used [17]. Back-projection algorithms are relatively unaffected by interpolation since no interpolation in the Fourier domain is required.

In this section, we first modify the fast back-projection algorithm to fit the far-field SAR scenario, and then compare it with the FFT-based algorithm using simulated data.

SAR data are frequency-offset Fourier data centered at frequency $\frac{2\omega_0}{c}$ [3]. To modify the fast back-projection algorithm to fit this scenario, the interpolations along radial directions should be adapted to be bandpass signal interpolations, while the projections are all assumed to be low-pass signals in CT images. Furthermore, since only one-sided Fourier data are known, the interpolators are complex-valued. The modified algorithm can be simply described as follows:

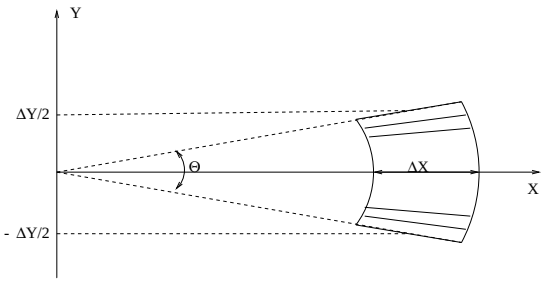

Figure 2. Far-field SAR data in 2-D FT domain.

1. Move the frequency-offset Fourier data to be centered at zero, and apply inverse FFT to obtain low-pass version of projections.
2. Shift and truncate the projections to correspond to small subimages.
3. Low-pass interpolate the projections in the radial direction to obtain new radial samples. Modulate all the projections by $e^{-j\frac{2\omega_0}{c}t}$.
4. Interpolate and decimate the modulated data to form half the number of projections.
5. Back-project along straight lines (approximation in far-field scenario) if in the last step of recursion. Otherwise, Multiply the projections by $e^{j\frac{2\omega_0}{c}t}$ and go back to step 2.

3.1 Simulation results for far-field scenario

We tested the fast algorithm with simulated data and compared the results with and an FFT-based algorithm. The basic simulation parameters are as follows:

- Center frequency: 10^{10} Hz. Data collection angle: 3^o.
- Same range and cross-range resolutions.
- Known data: 2N $\times$ 2N (angle$\times$ frequency) with image size N.
- Distance between the flight path and the center of the image is 100 times the image size.

The data collection angles were assumed to be uniformly distributed. The scene was simply four point targets with the same reflectivity magnitudes. Since the targets were far from the flight path, the data were treated as samples of the 2-D Fourier transform of the scene. The interpolation kernels in the FFT-based method were separable with Hamming-sinc interpolators in one direction, and simple linear interpolation in the other direction, since data in the angular direction was nonuniform. We first used a Hamming-sinc interpolator of length 8 in the FFT method and compared with our fast back-projection algorithm for different image sizes. The CPU time (in seconds) is shown in Table 1. From the table, we see that for different image sizes, the cost of the fast back-projection algorithm and the cost of the FFT method are of the same order with the ratio of the costs constant. The fast algorithm is about 10 times faster than the exact FBP algorithm for a 512×512 image and is more than 20 times faster than the exact FBP for a 2048×2048 image.

Table 1. Comparison of CPU time of IFFT and fast back-projection methods

Time \ Size	128	256	512	1024	2048
IFFT	1.34	6.16	29.63	154.5	866.7
Fast FBP	9.18	41.9	186.8	828.1	3635
Exact FBP	28.40	222.9	1778.9	14486	87033

To do a more meaningful comparison, we increased the length of Hamming-sinc interpolator in the FFT method to make the two algorithms have the same computational time. We show the reconstructed images of size 128 in Figs. 3 and 4. Both methods work very well in the far-field scenario with similar image quality.

4 Near-field SAR imaging

In the near-field scenario, wavefront curvature cannot be neglected. We have proven that the half-size half-bandwidth (of the flight path) property holds asymptotically in the near-field case, so that the fast algorithm can be modified to fit the near-field situation by doing the filtered back-projection on curves. That will be the topic of a forthcoming paper. Here, we will show some simulation results to verify the feasibility of our algorithm.

We first ran the simulations on the point targets under the same assumptions, except the distance between the flight path and the scene was now set to be 10 times the image size. We assumed that the pulse transmission points along the flight path were uniform, rather than using uniformly-spaced angles. In the FFT method, we used 2-D separable Hamming-sinc interpolation with the same filter length in each direction. The interpolator length was set to make the two methods have the same computational time. As shown in Figs. 5 and 6, the point targets reconstructed from the FFT method caused blurring due to the wavefront curvature, but the fast back-projection algorithm result was not affected.

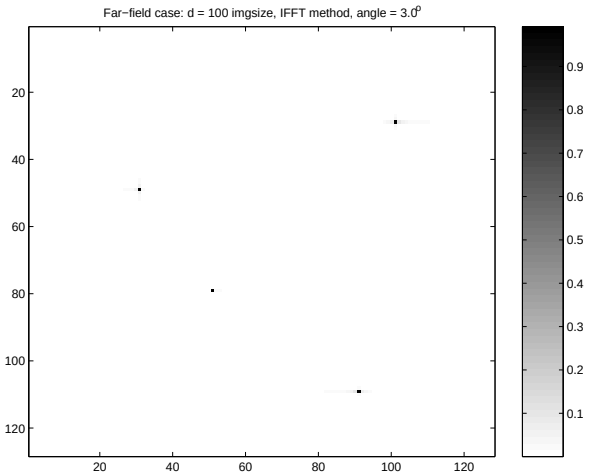

Figure 3. Far-field SAR image reconstruction using the FFT method with viewing angle 3^o.

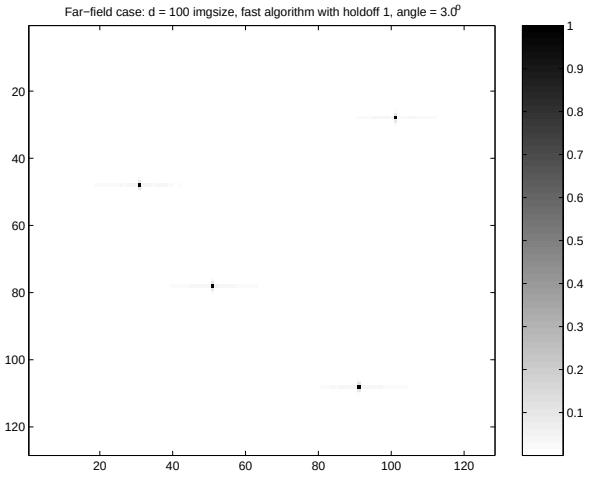

Figure 4. Far-field SAR image reconstruction using back-projection with viewing angle 3^o.

We also performed a simulation for a more complicated scene with four rings, each having the same inner and outer radius and centered at the four points appeared in the far-field simulation. The magnitudes of the reflectivities on the ring were set to be constant and the phases were simulated as random [18]. The distance between the flight path and the scene was assumed to be the same as the image size. The integration angle was from -27^o to 27^o. We show the results of using the FFT-based method and our modified fast back-projection algorithm. As illustrated in Figs. 7 and 8, the image produced by the FFT method has poor quality with smeared and shifted rings, while the fast back-projection algorithm formed excellent images with the same CPU cost.

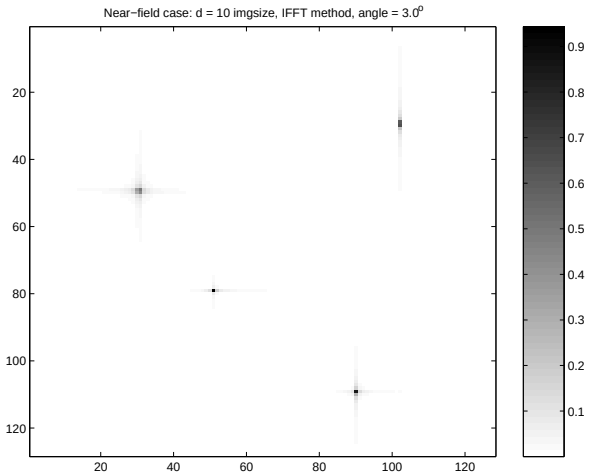

Figure 5. Near-field SAR image reconstruction using the FFT method with viewing angle 3^o.

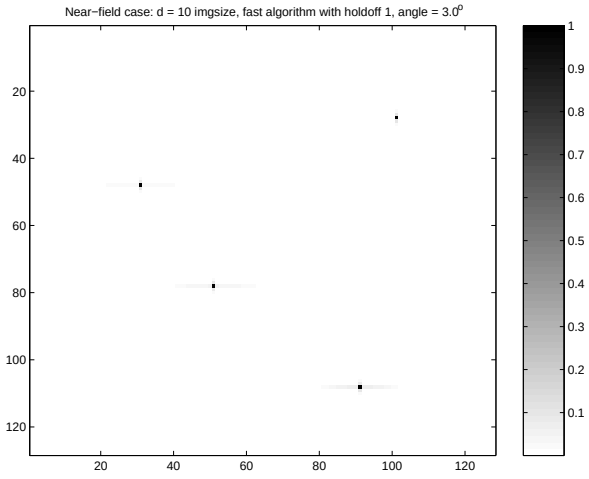

Figure 6. Near-field SAR image reconstruction using back-projection with viewing angle 3^o.

5 Conclusion

In this paper, we proposed a fast back-projection algorithm for the far-field scenario, which is a modification of a newly proposed fast back-projection algorithm in computer tomography. Our algorithm has the same order of computational cost as that of FFT-based algorithms. The quality of reconstructed image for the near-field scenario using fast back-projection can be better compared to that of the FFT method, while having the same CPU cost.

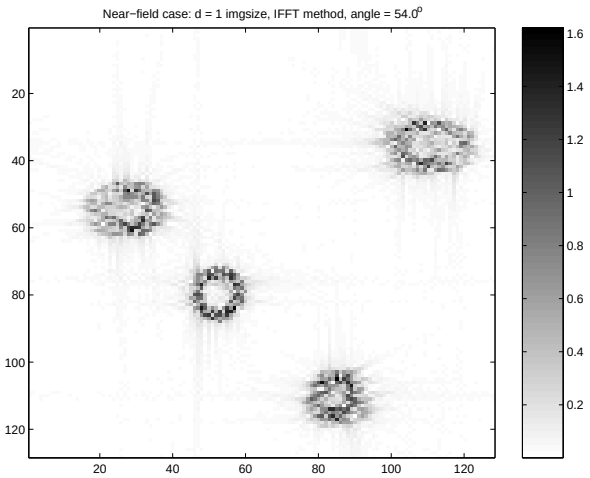

Figure 7. Near-field SAR image reconstruction using the FFT method with viewing angle 54^o.

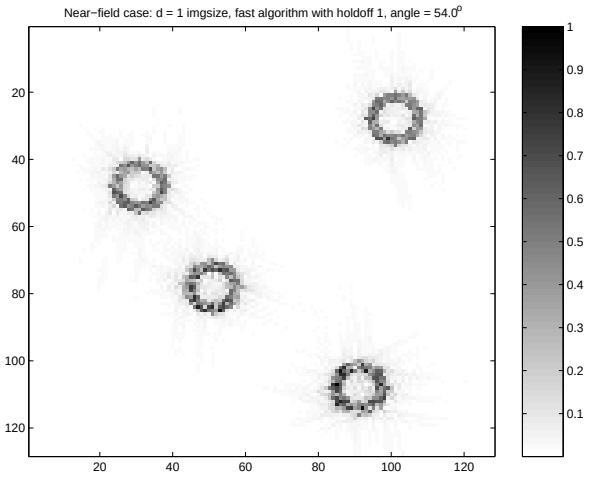

Figure 8. Near-field SAR image reconstruction using back-projection with viewing angle 54^o.

References

[1] A. Boag, Y. Bresler, and E. Michielssen. A multilevel domain decomposition algorithm for fast $O(N^2 \log N)$ reprojection of tomographic images. *Submitted to the IEEE Trans. on Image Processing.*

[2] S. Basu and Y. Bresler. Fast filtered hierarchical backprojection algorithm for tomography. *Submitted to the IEEE Trans. on Image Processing.*

[3] D. C. Munson, Jr, J. D. O'Brien, and W. K. Jenkins. A tomographic formulation of spotlight-mode synthetic aperture radar. *Proceedings of the IEEE*, 71(8):917–925, Aug. 1983.

[4] H. Choi and D. C. Munson, Jr. Direct-Fourier reconstruction in tomography and synthetic aperture radar. *International Journal of Imaging Systems and Technology*, 9:1–13, Jan. 1998.

[5] A. S. Milman. SAR imaging by $\omega - k$ migration. *International Journal of Remote Sensing*, 14(10):1965–1979, 1993.

[6] H. Choi, J. A. Lee, and D. C. Munson, Jr. On the wavenumber model in synthetic aperture radar. *Submitted to the IEEE Trans. on Image Processing.*

[7] S. Deans. *The Radon Transform and Some of its Applications*. Wiley, New York, 1983.

[8] P. A. Rattey and A. G. Lindgren. Sampling the 2-D radon transform. *IEEE Trans. on Acoustic, Speech, and Signal Processing*, 29(5):994–1002, Oct. 1981.

[9] F. Natterer. *The Mathematics of Computerized Tomography*. Wiley, Chichester, UK, 1986.

[10] A. G. Ramm and A. I. Katsevich. *The Radon Transform and Local Tomography*. CRC, Boca Raton, Florida, 1996.

[11] S. Basu and Y. Bresler. An analysis of errors in fast hierarchical backprojection. *Will submit to the IEEE Trans. on Image Processing.*

[12] J. McCorkle and M. Rofheart. An order $N^2log(N)$ backprojection algorithm for focusing wide-angle wide-bandwidth arbitrary-motion synthetic aperture radar. *SPIE Vol. 2747*, pages 25–36, 1999.

[13] J. L. Walker. Range-doppler imaging of rotating objects. *IEEE Trans. on Aerospace Electronic Systems AES-16*, pages 23–52, 1980.

[14] H. Stark, J. Woods, P. Indraneel, and P. Hingorani. An investigation of computerized tomography by direct Fourier inversion and optimum interpolation. *IEEE Trans. on Biomed. Eng.*, 28(7):496–505, 1981.

[15] N. Niki, T. Mizutani, and Y. Takahashi. A high-speed computerized tomography image reconstruction using direct two-dimensional Fourier transform method. *Syst.-Comput.-Contr.*, 14(3):56–65, 1983.

[16] H. Peng and H. Stark. Direct Fourier reconstrucion in fanbeam tomography. *IEEE Trans. on Med. Imaging*, 6(3):209–219, 1987.

[17] D. C. Munson, Jr. and J. O'Brien. An analysis of artifacts due to Fourier domain interpolation. *Twentieth Asilomar Conference on Signals, Systems and Computers*, pages 82–85, 1987.

[18] D. C. Munson, Jr. and J. L. Sanz. Image reconstruction from frequency-offset Fourier data. *Proceedings of IEEE*, 72(6):661–669, June 1984.